◆ Human Brain Mapping 34:2929–2943 (2013) ◆

Theta Power During Encoding Predicts Subsequent-Memory Performance and Default Mode Network Deactivation

Thomas P. White,[1,3] Marije Jansen,[1] Kathrin Doege,[1] Karen J. Mullinger,[2] S. Bert Park,[1] Elizabeth B. Liddle,[1] Penny A. Gowland,[2] Susan T. Francis,[2] Richard Bowtell,[2] and Peter. F. Liddle[1]*

[1]*Division of Psychiatry, University of Nottingham, Queen's Medical Centre, Nottingham, United Kingdom*
[2]*Sir Peter Mansfield Magnetic Resonance Centre, School of Physics and Astronomy, University of Nottingham, University Park, Nottingham, United Kingdom*
[3]*Department of Psychosis Studies, Institute of Psychiatry, King's College London, United Kingdom*

Abstract: The subsequent memory paradigm, according to which cerebral activity for later remembered (LR) and later forgotten (LF) items is contrasted, can be used to characterize the processes necessary for successful memory encoding. Previous simultaneous electroencephalography/functional magnetic resonance imaging (EEG/fMRI) memory studies suggest an inverse relationship between frontal theta band power and the blood oxygenation level dependent (BOLD) signal in the default mode network (DMN). The principal aim of this EEG/fMRI study was to test the hypothesis that this putative theta-DMN relationship is less evident in LF compared with LR trials. Fourteen healthy participants performed an episodic memory task in which pictorial stimuli were presented during encoding, and categorized (as LR or LF) by subsequent memory performance. For each encoding trial, the mean of the Hilbert envelope of the theta signal from 400 to 800 ms after stimulus presentation was calculated. To integrate the EEG and fMRI data, general linear models (GLMs) were used to assess the extent to which these single-trial theta values (as modulators of the main effect of stimulus) predicted DMN BOLD signal change, using: (i) whole-head univariate GLMs and (ii) GLMs in which the outcome variable was the time-course of a DMN component derived from spatial independent component analysis of the fMRI data. Theta was significantly greater for LR than LF stimuli. Furthermore, the inverse relationship between theta and BOLD in the DMN was consistently stronger for LR than LF pictures. These findings imply that theta oscillations are key to attenuating processes which may otherwise impair memory encoding. *Hum Brain Mapp 34:2929–2943, 2013.*

Key words: EEG; fMRI; memory; theta; default mode network

Additional Supporting Information may be found in the online version of this article.

Contract grant sponsor: Medical Research Council; Contract grant number: G0601442.

*Correspondence to: Peter. F. Liddle, Division of Psychiatry, University of Nottingham, A Floor, South Block, Queen's Medical Centre, Nottingham NG7 2UH, United Kingdom.
E-mail: peter.liddle@nottingham.ac.uk

Received for publication 11 January 2011; Revised 28 February 2012; Accepted 3 April 2012
DOI: 10.1002/hbm.22114
Published online 19 June 2012 in Wiley Online Library (wileyonlinelibrary.com).

INTRODUCTION

Great variability exists in the degree to which we later remember events despite their apparent experiential similarity. Neural activity at the time of sensory experience is crucial to the encoding process. Successful encoding is contingent upon the translation of sensory percepts to internal representations which are in turn bound into accessible, enduring traces in the subjective environment [Paller and Wagner, 2002]. Behavioral evidence suggests that multiple interacting factors shape encoding: attention, novelty, and emotional arousal all modulate memory performance [Canli et al., 2000; Kelley et al., 1998; Murdock, 1960]. Memory formation relies on the modification of synaptic connections. This modification or plasticity is more likely at times of coordinated activity of neural populations [Buzsaki and Draguhn, 2004]. This coordinated activity typically increases the power of oscillations observable in data recorded using electroencephalography (EEG). Increased oscillations in the theta band (3–8 Hz) have been robustly reported during memory processing. Observed associations between frontal midline theta oscillations and cognitive load in spatial learning, spatial navigation, verbal, and spatial working memory and item recognition [Gevins et al., 1997; Jensen and Tesche, 2002; Onton et al., 2005; Weidemann et al., 2009], suggest that theta oscillations play a generalized role in memory processing.

Key to the experimental examination of memory encoding is the subsequent memory (SM) paradigm, in which neural responses to specific events are recorded and categorized according to a later retrieval test, thus providing a measure of differential neural activity according to memory performance [Paller and Wagner, 2002]. Klimesch et al. [1997] reported SM effects on the theta power measured over frontocentral midline electrodes during a verbal memory test. Increased theta coherence between frontal and posterior electrodes has also been observed for later remembered (LR) compared with later forgotten (LF) words [Weiss et al., 2000]. This literature highlights the utility of frontal midline theta in SM prediction. Intracortical recordings have identified neuroelectric SM effects in other brain structures. It has been recently observed, from electrodes implanted within the hippocampus and amygdala of presurgical eplilepsy patients, that the strength of phase-locking of local field theta oscillations to single neuron spikes predicts episodic memory performance [Rutishauser et al., 2010]. This observation provides a mechanistic explanation of plasticity-induced changes in task-related oscillations observed at the scalp. Furthermore, there is growing evidence in favor of cross-spectral SM effects, particularly between theta and gamma (>25 Hz) oscillations. The strength of theta-gamma comodulation in CA3 of the rat hippocampus of item-context learning has been found to increase as memory performance increases [Tort et al., 2009]. This finding concurs with the work of Sederberg et al. [2003], who used subdural recording in humans, and observed concomitant SM effects in post-stimulus theta and gamma in right frontal and temporal cortex electrodes. In a magnetoencephalography study, Osipova et al. [2006] used a pictorial episodic memory task and similarly observed SM effects specific to theta and gamma in response to pictures, with these effects being maximal in parietal regions between 300 and 1,200 ms post stimulus.

Blood oxygenation level dependent functional magnetic resonance imaging (BOLD fMRI) has also been used to investigate SM effects. Wagner et al. [1998] found greater activity for LR than LF words in left inferior prefrontal and fusiform cortex and medial temporal lobe regions. Brewer et al. [1998] found comparable, but right-lateralized SM effects when studying complex visual scenes. SM effects of increased amygdala activation have also been observed in response to emotionally arousing scenes [Canli et al., 2000]. An important finding was also made by Otten and Rugg [2001], who reported that regions including the medial parietal, dorsolateral prefrontal cortex, and bilateral angular gyrus were more activated during the encoding of LF compared with LR words. This finding bucked the trend for a positive relationship between activation and SM performance and suggested that activation in these areas actually impaired effective encoding. Daselaar et al. [2004] found differential activity in a similar pattern of regions, but crucially proved that their findings could be attributed to an error-related attenuation of patterns of deactivation shown during successful encoding. Recently, Anticevic et al. [2010] used a working memory task with distractor stimuli presented in the maintenance phase to identify two networks with dissociable functional roles and in both of which increased deactivation of activity at the time of encoding was predictive of better memory performance. The first of these, the default mode network [DMN; Raichle et al., 2001] is an intrinsically correlated, distributed network typically comprising medial frontal, precuneus, posterior cingulate and bilateral angular gyrus, and has consistently been shown to be deactivated during cognitive task performance and preferentially activated at times of rest and introspection [McKiernan et al., 2003; Raichle et al., 2001]. Suppression of activity here and concomitant attentional allocation to encoding-relevant regions provides a simple explanation for previous results [Daselaar et al., 2004; Otten and Rugg, 2001]. The second preferentially deactivated network identified by Anticevic et al. [2010] was found bilaterally at the temporoparietal junction (TPJ), spanning principal regions of the ventral attention network [VAN; Corbetta et al., 2002], which is activated by behaviorally salient stimuli acting to orient attention to the external environment. Suppression of this region may aid goal-directed task performance by reducing interference effects of distractor stimuli. In summary, it is increasingly clear that successful memory formation relies not only on preferential activation of structures directly related to memory processes, but also on preferential deactivation of task-irrelevant structures.

Concurrent acquisition of EEG and fMRI data (EEG/fMRI) provides a means of noninvasively resolving the

temporal and spatial characteristics of brain activity, while controlling for attention, training, and habituation effects associated with the independent acquisition of EEG and fMRI data. It is therefore a potentially valuable technique for consolidating oscillatory and hemodynamic SM findings. However, it should be stressed that the eradication of artifacts in EEG recordings made during concurrent fMRI, including those due to cardio-ballistic effects and the MR-gradients, remains a challenge. Several techniques have been developed to improve artifact correction through both optimized image acquisition and postprocessing [Allen et al., 1998, 2000; Mullinger et al., 2008] and the successful use of simultaneous EEG/fMRI to investigate regional activity associated with neural oscillations and their cognitive modulation relies on the elimination of these artifacts.

Simultaneous EEG/fMRI has been used to reveal a putative negative relationship between variations in frontal midline theta oscillatory power and DMN BOLD activity both during cognitively demanding working memory tasks and at rest. Scheeringa et al. [2008] employed independent component analysis (ICA), a data-driven blind-source separation method that identifies spatial patterns on the basis of their maximal temporal independence, to define a frontal midline theta component of EEG data acquired during rest. Using a general linear model (GLM) approach, and a regressor created by convolving continuous theta values with the canonical hemodynamic response function (HRF), they observed that fluctuations in convolved theta power were significantly negatively correlated with BOLD signal in the DMN, and that there were no significant positive correlations in any brain region. Developing this approach to investigate the effect of task-related theta, Scheeringa et al. [2009] observed that theta-related variation in the maintenance period of a Sternberg working memory task was similarly negatively correlated with DMN BOLD activity. Michels et al. [2010] also reported an inverse relationship between single-trial theta and DMN BOLD during working memory retention. Despite growing evidence of a theta-DMN relationship, details of its modulation by memory performance are yet to be reported. Here, we investigate subsequent episodic memory effects in simultaneously-acquired EEG/fMRI data with the aim of addressing three principal hypotheses:

1. memory encoding performance as judged by a later retrieval test can be predicted from single-trial frontal midline theta power measured during encoding;
2. variation in this single-trial theta value is negatively correlated with the BOLD signal within regions that together comprise the DMN, including medial prefrontal, posterior cingulate, precuneus, and bilateral angular gyrus; and
3. the robustness of the hypothesized theta-DMN relationship will be stronger for correctly compared with incorrectly remembered items.

METHODS

Participants

All subjects gave informed written consent prior to participation in this study, which was approved by our local ethics committee and performed in compliance with the Declaration of Helsinki. Twenty-two participants were recruited to take part in an episodic memory fMRI experiment. Incomplete data were collected for four participants: two aborted the scan session; and two were excluded as corruption of the EEG marker data-files prevented data analysis. During analysis a further four participants were excluded because, after rejecting artifactual trials on the basis of the EEG data, there remained fewer than 10 error trials. This was considered too few to construct a meaningful time-frequency average for LF trials or assess theta SM effects. The final study group therefore consisted of 14 participants [6 males, 28 $\pm$ 8 years (mean age $\pm$ standard deviation)]. All participants had normal sight or sight that was corrected to normal using the optic fiber goggle system employed during the fMRI study. Participants reported no history of mental illness or neurological injury and were not prescribed medication at the time of study.

Experimental Task

The experimental task was a shortened version of the episodic-memory task described by Gruber et al. [2008] which was programmed using Presentation (Neurobehavioral Systems, USA). Subjects took part in two 16-min sessions of the task, which is illustrated schematically in Figure 1. Totally, 250 colored pictures of "living" or "non-living" objects were selected from a standard picture library (Hemera Photo-Objects 5000). Fifty of these were used exclusively for training purposes and 200 for the fMRI experiment. Pictures used in the first session were excluded from the second session. Each session comprised a 6.5-min encoding phase, followed by a 30-s rest period and a 9-min retrieval phase. All visual stimuli were presented using an optic fiber goggle system (Nordic Neuro Lab, Norway). Participants were instructed to attend to a central fixation cross at all interstimulus periods. The encoding phase comprised 40 trials. Each began with presentation of a randomly selected picture for 1.2 s on a black background in either the top or bottom half of a grid. Directly after stimulus presentation, participants were presented with the question: "living or non-living?" for 1.5 s, during which time they were required to make a button-press judgment. Each trial finished with a rest period of a pseudo-randomly assigned duration of between 3 and 5 s. The retrieval phase consisted of 60 trials. Each trial began with one of 60 pictures (40 shown in the encoding phase, 20 new) being presented for 2 s in the center of the screen. Participants were then presented with an empty grid to which they were required to make a source and retrieval judgment within 2 s. For pictures judged

Figure 1.

Illustrative schematic of task, depicting the stimulus timings of an encoding-phase trial (top) and a retrieval-phase trial (bottom). [Color figure can be viewed in the online issue, which is available at wileyonlinelibrary.com.]

"old," a trackerball (fORP, Cambridge Instruments, UK) was used to move a cursor from the mid-point of the screen to the section of the grid in which the picture was remembered to have been in the encoding phase. A button was then pressed. All button responses were performed with the right index finger. For pictures judged "new," the trackerball was used to move the cursor to the exterior of the grid and the button similarly pressed. A rest period of duration 3–5 s concluded the retrieval trials. To ensure sufficient sampling of the BOLD signal baseline, 10 additional null trials of a pseudo-randomly determined duration of 10–15 s were included in both the encoding and retrieval phases.

MRI Data Acquisition

Blood oxygenation level-dependent (BOLD) datasets were acquired on a 3 Tesla Philips Achieva MRI scanner (Philips, Netherlands). To enhance sensitivity, dual-echo gradient-echo echo-planar images (GE-EPI) were acquired [Gowland and Bowtell, 2007; Posse et al., 1999], using an eight-channel SENSE head coil with SENSE factor 2 in anterior–posterior direction, TE_1/TE_2 20/48 ms, flip angle 85°, 255 × 255 mm field of view, with an in-plane resolution of 3 mm × 3 mm and a slice thickness of 4 mm, and TR 3,000 ms. At each dynamic time point a volume dataset was acquired consisting of 40 contiguous axial slices acquired in descending order. The number of slices and TR were selected to facilitate synchronization of the EEG and scanner clocks [Mandelkow et al., 2006]. Totally, 330 dynamic time points were acquired during the entire fMRI paradigm. A magnetization prepared rapid acquisition gradient echo image with 1mm isotropic resolution, 256 × 256 × 160 matrix, TR/TE 8.1/3.7 ms, shot interval 3 s, flip angle 8°, SENSE factor 2 was also acquired for each participant for image registration.

Electrophysiological data acquisition

EEG data from 31 scalp electrodes positioned according to the international 10–20 system of electrode location were recorded with an MR-compatible electrode cap equipped with Ag/AgCl electrodes (Braincap MR, Brain Products, Germany). An additional electrode was placed under the right eye to monitor eye movements. The upper-limit of electrode impedance was 10 kΩ. EEG data were digitized and amplified using an MR-plus amplifier (Brain Products, Germany) and recorded using Brain Vision Recorder (BVR; Version 1.10, Brain Products, Germany) with a 5 kHz sampling rate. Acquisition of EEG data was synchronized with MR data acquisition (Syncbox, Brain Products, Germany) and scanner trigger pulses were lengthened to facilitate their recording with BVR. Presentation event codes were additionally imported into the BVR data file. ECG data were acquired using an MR-compatible four-channel vector cardiogram system (VCG; Philips, Netherlands) and sampled at 500 Hz [Chia et al., 2000]. Respiratory data were recorded using an MR-scanner

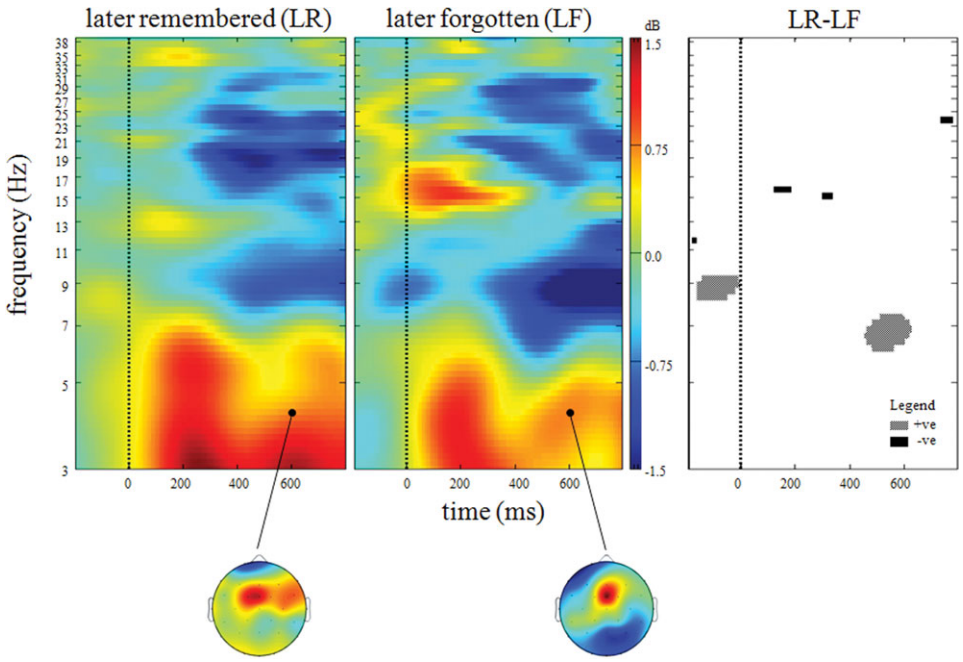

Figure 2.

Group time-frequency plots for visual stimuli presented during encoding and classified on the basis of subsequent memory performance. Left shows data for later remembered (LR) while middle shows later forgotten (LF) pictures. Right shows time-frequency points where significant ($P < 0.01$ uncorrected) subsequent memory effects were observed. All data presented were measured at FCz. Color-bar depicts power at each time-frequency point. Scalp maps depict power distribution at the demarcated time-frequency point. [Color figure can be viewed in the online issue, which is available at wileyonlinelibrary.com.]

pneumatic belt (Philips, Netherlands) and sampled at 500 Hz.

Data Analysis

EEG pre-processing and primary analysis

Gradient artifacts were cleaned from EEG data using average artifact subtraction [Allen et al., 1998, 2000] in Brain Vision Analyzer (Version 1.05, Brain Products, Germany). Data were then band-pass filtered between 0.1 and 40 Hz, with an additional notch filter applied at 50 Hz to remove the mains-artifact. R-peak markers derived from the VCG were aligned with the EEG data [Mullinger et al., 2008]. Data were then down-sampled to 250 Hz and imported into EEGlab [Delorme and Makeig, 2004] for pulse artifact correction by means of optimal basis sets within the fMRIB plugin [Niazy et al., 2005], using the VCG derived R-peak markers. To eliminate eye movements, an automatic electro-oculargram artifact correction method using blind source separation was applied (AAR toolbox, EEGlab plugin; http://www.cs.tut.fi/~gomezher/projects/eeg/index.htm). Single-trial data were calculated by segmenting from 1,000 ms pre- to 1,996 ms post-presentation of the encoding picture, with events classified on the basis of the SM test as being either LR or LF pictures. LF pictures included both those pictures for which the location was incorrectly remembered and those which were incorrectly designated as new. Analysis focused upon EEG data recorded at FCz because of the sensitivity of this site to SM effects [Klimesch et al., 1997]. Events containing within-event voltage differences exceeding 50 μV were excluded, as were trials deemed improbable because they exhibited a relative kurtosis exceeding five standard deviations.

Visualization of the data in time-frequency space was afforded by the calculation of LR- and LF-specific event-related spectral perturbations [ERSPs; Makeig, 1993] using EEGlab [Delorme and Makeig, 2004]. This technique calculates the power (dB) at a given frequency and latency relative to a time-locking event of interest, which was in this instance the presentation of the encoding stimuli. Within each of 100 frequency bins from 3 to 40 Hz, event-related shifts in the power spectrum were assessed using a wavelet comprising three cycles of a sinusoidal wave at the central frequency of the bin. The use of variable cycle length permits better frequency resolution at high frequencies than techniques using constant cycle length [Delorme and Makeig, 2004]. Single-trial ERSPs were calculated from 1,000 ms pre- to 1,996 ms post-stimulus, averaged across trials and averaged across participants. Group-averaged ERSPs (Fig. 2) revealed distinct early (0–400 ms after stimulus presentation) and late (400–800 ms) frontomedial

theta increases (3–7.5 Hz). This frequency range was therefore used to represent theta. Statistical comparison (of LF-LR) confirmed previous reports that SM effects were maximal in this later window [Osipova et al., 2003]. On this basis, single-trial theta values in the later time window were recorded and used for integrating EEG and fMRI analyses.

Single-trial theta was calculated by first band-pass filtering cleaned EEG data recorded at FCz between 3 and 7.5 Hz, using a two-way least squares finite impulse response filter, and then baseline-correcting between −200 and 0 ms, with this baseline averaged across both trial types to minimize the influence of between-condition differences in prestimulus activity on poststimulus measures. Hilbert transforms provide a measure of amplitude modulation of oscillatory processes. The mean of the Hilbert envelope of theta from 400 to 800 ms was recorded for each event. Theta values were Z-transformed (prior to categorization) for use in later EEG/fMRI integratory analyses to assess differential memory effects.

Alternative methods of assessing single-trial theta oscillatory activity for subsequent EEG/fMRI integratory analysis include projecting the EEG data into source-space or characterizing multivariate features of the EEG signal in whole-scalp topographies. For example, ICA of EEG data has been previously used with success in this context [Scheeringa et al., 2009]. Discussion of an ICA-derived theta EEG/fMRI analysis is presented as Supporting Information 1 and Supporting Information Figure 1.

fMRI: preprocessing, general linear models, and independent component analysis

fMRI data preprocessing was performed using SPM8 (Statistical Parametric Mapping, Wellcome Department of Imaging Neuroscience, University of London, UK). Data were corrected for slice-timing differences and spatially realigned. Movement parameters were assessed for each participant, and participants were excluded if movement exceeded 3 mm. A single dataset was produced from a weighted summation of the dual-echo dynamic time course [Gowland and Bowtell, 2007; Posse et al., 1999]. Retrospective physiological correction of this dataset was then performed (RETROICOR; Glover et al., 2000), before coregistration of the dataset with subject-specific anatomical MR data, normalization to SPM template and spatial smoothing using a Gaussian kernel with a 5 mm full width at half maximum. A high-pass temporal filter was applied to minimize effects of low-frequency physiological and scanner-derived confounds.

First-level, event-related analyses were performed using individually specified general linear model (GLM) design matrices, which modeled the time course of the BOLD response associated with the presentation of the visual stimuli, by convolving a series of rectangles of 2 sec duration with the canonical hemodynamic response function. Two regressors (per session) were included for encoding stimuli, which were categorized as LR or LF stimuli; two regressors were included for the retrieval stimuli, which were categorized as those presented in the encoding phase and those new to the retrieval phase. Regressors for the temporal derivatives of each of these predictors were also included to allow for the possibility of small latency variations in the activated areas. Realignment parameters were included in the GLMs as covariates of no interest. From these models, first-level contrast images for the activation related to LR and LF stimuli were calculated and entered into second-level random effects analyses.

In a further analysis, group spatial independent component analysis (ICA) was performed on the preprocessed BOLD data (Infomax algorithm; GIFT toolbox; http://icatb.sourceforge.net). Twenty spatial components were identified. Spatial correlation of these components with the DMN mask incorporated within GIFT was assessed. All components with a significant spatial correlation ($P < 0.05$) with the DMN were further investigated in relation to theta oscillatory activity (as is described in Section EEG/fMRI data integration).

EEG/fMRI data integration

A whole-head univariate GLM analysis was performed to test the hypothesis that trial-by-trial theta variation predicted BOLD signal changes more strongly for LR than LF events. This was achieved by including single-trial theta values, calculated as described above (Section EEG preprocessing and primary analysis), as parametric modulators of the LR and LF stimuli in models otherwise identical to those described above (Section fMRI: preprocessing, general linear models, and independent component analysis). A session-specific mean value was entered as the parametric modulator value for those trials identified as being artifactual in the EEG analysis. For each participant, a contrast image was computed to evaluate whether there were any regions whose activity was predicted by theta variation in relation to LR stimuli. Equivalent contrast images were also computed to assess the effect of theta variation in relation to LF stimuli. In addition, contrast images were computed to test whether theta differentially predicted BOLD for LR and LF events by subtracting the effect of theta related to one encoding stimulus class from the effect of theta related to the other. These contrast images were then included within second-level random-effects analyses to test the hypothesis that theta variation predicted BOLD activity for the group. Both positive and negative correlates of theta were examined throughout the analysis.

To assess explicitly the relationship between single-trial theta and BOLD activity in the DMN while minimizing the problem of multiple comparisons inherent in whole-head, univariate voxel analyses, regression analyses were performed on the multiple spatial components that significantly correlated with the DMN mask provided by GIFT using the same design matrices as those used in the univariate EEG/fMRI analysis described above. The DMN mask in GIFT is a whole-brain weighted *Z*-score image

TABLE I. Task performance

	Response			
	Correct		Incorrect	
Judgment	%	RT (s)	%	RT (s)
Encoding	96.7 (1.7)	0.62 (0.11)	3.3 (1.7)	1.03 (0.46)
Retrieval	69.7 (9.5)	0.95 (0.12)	30.3 (9.5)	0.88 (0.10)

Accuracy of response during the encoding and retrieval phases of the episodic memory task. Response times (RTs) are given as the group-mean of the single-subject median results. Values in brackets denote the standard deviation.

with *Z*-score peaks in core DMN regions including the precuneus, bilateral angular gyrus, and ventral and superior medial PFC. Resulting beta values associated with LR stimulus effect, LF stimulus effect, LR stimulus theta, and LF stimulus theta were recorded for each individual. One sample *T*-tests were performed for each of these variables for each DMN component so as to assess whether the regression coefficients for these variables differed from zero for the group.

To assess whether these beta values differed according to SM performance and/or the DMN component being investigated, two repeated-measures analysis of variance (rmANOVA) analyses were performed. In the first, beta values for LR stimulus and LF stimulus were entered for all DMN components. Using SM performance and independent component as within-subject factors, this rmANOVA tested whether beta values associated with the stimulus differed according to memory performance and/or according to the DMN component in question.

In a second rmANOVA analysis, beta values for LR stimulus theta and LF stimulus theta were entered, again using SM performance and DMN component as within-subject factors, this rmANOVA tested whether the theta prediction of DMN activity differed according to SM performance and/or the DMN component in question.

RESULTS

Behavior

Participants performed with a mean accuracy of 96.7% in the encoding judgment and 69.7% in the subsequent retrieval test. For the encoding period, response times (RTs) for the correct responses were significantly shorter than those for incorrect responses ($T(13)=3.30$, $P = 0.003$). No significant SM difference in RT was observed in the retrieval judgment. Behavioral results are summarized in Table I.

Frontal Theta SM Effects

Figure 2 illustrates group mean time-frequency power changes at FCz for LR and LF stimuli. Increased theta power is evident for both LR and LF stimuli from 0 to 400 ms post stimulus with no significant between-condition differences. In a later window from 400 to 800 ms significant SM effects are observed with increased theta power for LR compared to LF stimuli. As is depicted in the right-hand portion of Figure 2, this effect is centered on 7 Hz from approximately 500–600 ms post stimulus. The scalp maps in Figure 2 depict the scalp distribution of theta power in this time window and highlight that this effect was focused on FCz. An additional significant SM effect was also observed at ~16 Hz from 100 to 300 ms post stimulus with LF exhibiting enhanced beta power when compared with LR pictures. The mean Hilbert-transformed 3–7.5 Hz signal between 400 and 800 ms post stimulus presentation was greater for LR than LF stimuli (LR theta: 1.43 ± 0.22 dB (mean ± standard deviation); LF theta: 1.24 ± 0.24 dB; SM effect: $T(13) = 2.84$, $P = 0.010$).

BOLD Correlates of Task

Both LR and LF stimuli elicited activation in a diverse cortical network including significant clusters within visual regions including bilateral lingual gyrus, in the supplementary motor area and cingulate cortex, and in bilateral inferior frontal gyrus (IFG) and bilateral thalamus (Table II and Fig. 3). Clusters included peak voxels in right parahippocampal gyrus for both stimulus types. Significant deactivation of medial frontal areas, precuneus and bilateral angular gyrus was observed in association with both stimulus types (Table II and Fig. 3). Whole-head examination of SM effects, derived from a contrast of LR-LF pictures, revealed no significant clusters at an uncorrected voxel-level threshold of $P < 0.05$. In light of the severe loss of statistical power due to the need for stringent correction for multiple comparisons in voxel-based analyses of the entire brain, a region of interest (ROI) analysis was conducted in limbic regions in which SM effects were demonstrated in a recent meta-analysis (Spaniol et al., 2009). This analysis is reported in Supporting Information 2 and indicates a trend for greater BOLD activation during LR compared with LF trials in the right amygdala.

Theta Modulation of BOLD

Univariate voxel-based analysis

The late theta signal during encoding exhibited a significant negative correlation with BOLD in the medial frontal gyrus during LR trials (Fig. 4a and Table III). In LF trials the correlation was less consistent (Fig. 4a). Explicit comparison of theta-BOLD relationships for LR and LF stimuli revealed a cluster centered in medial frontal gyrus where this SM difference was observed to be significant (Fig. 4b and Table III). The whole-brain analysis revealed no regions in which the theta signal exhibited a significant positive correlation with BOLD in either trial type. In the ROI analysis of the right amygdala described in

TABLE II. Selected foci of task-induced activation and deactivation in response to later remembered (LF) and later forgotten (LF) stimuli during encoding

Contrast	Region (Brodmann area)	MNI coordinates			Local maximum
		X	*Y*	*Z*	*T*-value
(A)Task-induced activations					
LR > baseline	Lingual gyrus (18)	16	−80	−10	11.05
	Lingual gyrus (18)	−14	−82	−12	9.93
	Middle occipital gyrus (19)	34	−84	16	9.97
	Fusiform gyrus (37)	34	−48	−18	9.79
	Inferior parietal lobule (40)	−44	−40	56	10.03
	Supplementary motor area (6)	4	0	62	6.88
	Cingulate cortex (32)	−8	12	40	6.54
	Inferior frontal gyrus (13)	36	22	8	6.83
	Inferior frontal gyrus (13)	−34	22	8	6.43
	Thalamus	−10	−12	6	5.94
	Thalamus	10	−14	0	7.36
	Parahippocampal gyrus (35)	30	−28	−22	7.17
LF> baseline	Lingual gyrus (18)	14	−80	−10	9.61
	Lingual gyrus (18)	−14	−82	−12	9.62
	Middle occipital gyrus (19)	28	−88	14	8.91
	Fusiform gyrus (37)	34	−48	−20	8.32
	Inferior parietal lobule (40)	−46	−40	56	6.82
	Supplementary motor area (6)	2	0	62	6.66
	Cingulate cortex (32)	−2	12	44	7.41
	Inferior frontal gyrus (13)	36	22	8	7.81
	Insula (13)	−28	26	6	5.03
	Thalamus	−10	−18	6	7.40
	Thalamus	12	−14	2	8.40
	Parahippocampal gyrus (30)	16	−46	−2	7.46
	Amygdala	30	−2	−22	4.89
(A) Task−induced deactivations					
LR < baseline	Anterior cingulate cortex (32)	−4	39	8	4.49
	Medial frontal gyrus (10)	10	50	2	4.18
	Superior frontal gyrus (9)	10	50	30	2.94
	Middle frontal gyrus (8)	−36	20	52	3.68
	Middle frontal gyrus (8)	36	28	48	5.40
	Angular gyrus (39)	−44	−70	36	4.55
	Angular gyrus (39)	52	−66	34	2.39
	Posterior cingulate cortex (31)	−8	−52	24	3.22
	Posterior cingulate cortex (31)	2	−50	28	3.67
LF < baseline	Medial frontal gyrus (10)	−4	58	14	6.41
	Superior frontal gyrus (9)	−4	52	30	4.03
	Middle frontal gyrus (8)	−30	28	50	4.35
	Middle frontal gyrus (8)	18	28	56	3.02
	Angular gyrus (39)	−48	−70	30	6.48
	Angular gyrus (39)	52	−64	36	3.25
	Posterior cingulate cortex (31)	−6	−44	38	3.02
	Precuneus (7)	−8	−62	30	3.83

T-values describe peak voxels within significant clusters of task-induced activation and deactivations.

Supporting Information 2, positive modulation of BOLD by theta was significantly greater for LR than LF stimuli.

DMN ICA analysis

Figure 5 depicts the three spatial components that correlated significantly with the DMN mask from GIFT. Component A, which exhibits a ring-like distribution on account of missing voxels in ventral prefrontal cortex caused by signal dropout due to susceptibility effects in this area, is centered on medial frontal gyrus (correlation with DMN: $R = 0.371$, $P < 0.01$); component B on medial and superior frontal gyrus, ACC, bilateral insula, and bilateral angular gyrus ($R = 0.563$, $P < 0.01$); and

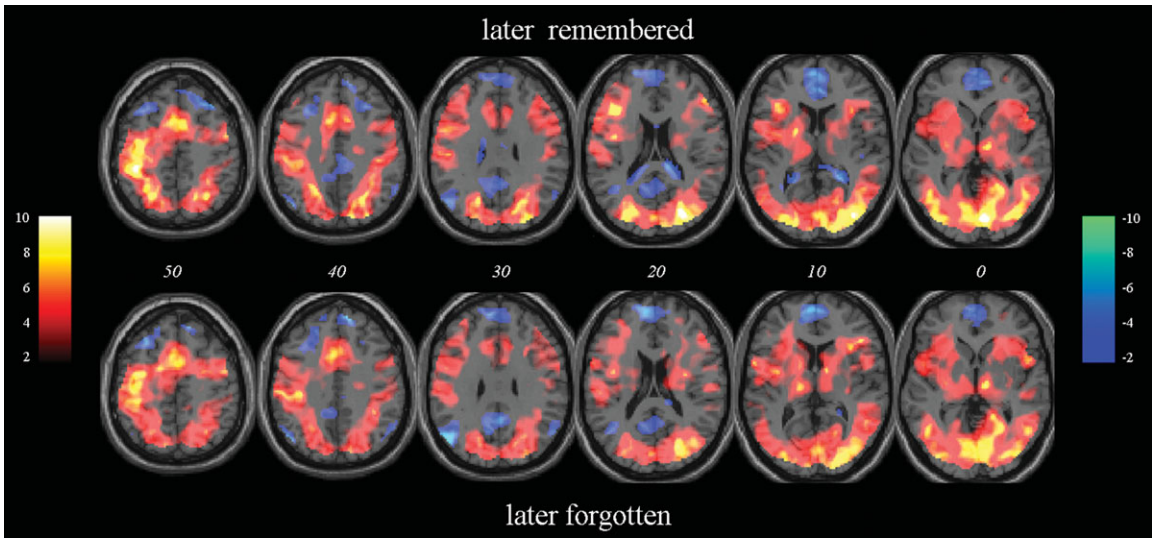

Figure 3.

Activation observed during processing of visual encoding stimuli relative to baseline. Random-effects group data for stimuli that are later remembered (LR; top) and later forgotten (LF; bottom) in the subsequent memory test. Both activations and deactivations presented are significant at uncorrected voxel threshold of $P < 0.001$. Data are overlaid on a standard averaged T1-weighted MR-image displayed according to neurological convention. Positive *T*-score values are defined in the colorbar located on the left, negative *T*-scores in the right-hand color-bar. Italicized numbers denote MNI Z co-ordinate of the axial slice shown. [Color figure can be viewed in the online issue, which is available at wileyonlinelibrary.com.]

component C on medial frontal gyrus, posterior cingulate cortex, precuneus, and bilateral angular gyrus ($R = 0.343$, $P < 0.01$). BOLD activity in these components was robustly observed to be negative in association with presentation of encoding stimuli irrespective of their subsequent memory (Table IV). rmANOVA revealed a significant within-subject effect of the component ($F(2,13) = 7.59$, $P = 0.007$), but no SM effect.

As with the whole-head univariate analysis, event-related theta signal significantly modulated the relationship between the trial event and BOLD signal during LR trials but exerted a significantly weaker modulatory effect during LF trials (Table IV). A significant negative relationship between late theta and DMN BOLD was only observed for LR stimuli, with the strongest relationship found for component B in response to these stimuli. The rmANOVA revealed an overall SM effect ($F(1,13) = 5.43$, $P = 0.037$), but no significant between-component effect. Similarly, despite some variation in the degree to which theta predicted BOLD for LR stimuli for the components studied, the overall (component × memory performance) interaction was not significant.

DISCUSSION

Concurrent EEG/fMRI recording during the execution of a cognitive task provides a unique means of studying the effect of a measurable behavioral manipulation on oscillatory activity, regional hemodynamic responses and the interaction of oscillatory and hemodynamic measures. A principal focus of the current study was the investigation of oscillatory power changes in the theta band during the encoding of pictorial stimuli. Frontal midline theta increases were observed during encoding, with these increases found to be significantly greater for LR compared to LF pictures. Investigation of time-frequency space showed a significant SM effect at ~7 Hz and a latency of 500–600 ms post stimulus presentation, while explicit examination of the mean theta signal between 400 and 800 ms post stimulus also confirmed greater theta power for LR than LF pictures. Frontal midline SM effects have previously been reported during word encoding [Klimesch et al., 1997; Weiss et al., 2000]. Furthermore, Osipova et al. [2003] reported parietal theta SM differences for pictorial stimuli to be maximal from 300 to 1,200 ms. The latency of our findings is therefore broadly congruent with previous observations.

Frontal theta power has previously been delineated as a marker of mental effort and increased attentional demands [Sauseng et al., 2007]. In addition, Luu and Tucker [2001] observed that theta power increased over somatomotor regions following known-error responses, while Makeig et al. [2004] found increased theta power directly following manual responses to target stimuli. These findings suggest that theta plays a role in context updating. Both directed attention and context updating are vital aspects of successful memory encoding. Increased frontal theta power for

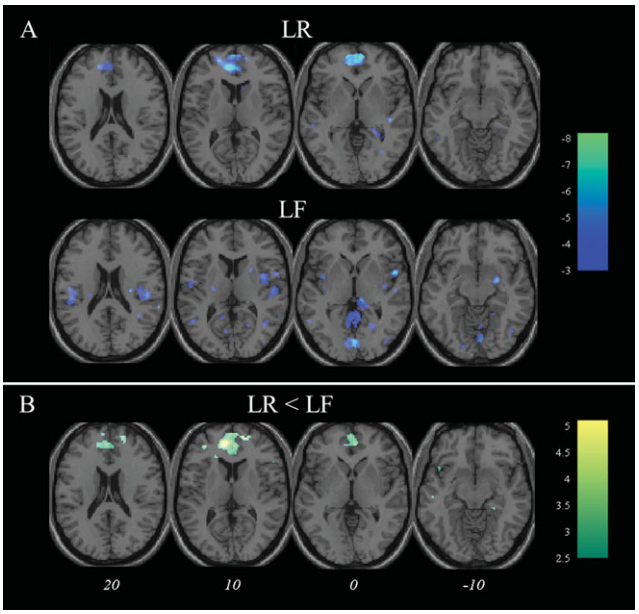

Figure 4.

Theta negatively predicts frontomedial blood oxygenation level dependent signal. **A**: Regions exhibiting a negative relationship with theta during encoding for later remembered (LR; top) and later forgotten (LF; bottom) pictures; (**B**) depicts regions exhibiting a more negative relationship with theta for LR compared to LF pictures. Images are overlaid onto a standard T1-weighted brain image. Color-bars denote *T*-values. Italicized numbers denote MNI Z co-ordinate for axial images above and apply to both sections of figure. [Color figure can be viewed in the online issue, which is available at wileyonlinelibrary.com.]

LR compared with LF pictures can be explained by these processes being more prevalent at times of LR stimulus presentation. It has been proposed that theta band oscillations underlie long-range communication between frontal midline and concurrently active brain regions [von Stein and Sarnthein, 2000]. Increased theta band coupling between frontal midline and posterior sensory regions has also been observed at times when a manual response requires increased integration of visual and sensory information [Sauseng et al., 2007]. In light of these findings, it is plausible that frontal theta acts to recruit other task-relevant regions. Furthermore, it could be argued that the increased theta power for LR pictures represents an increased capacity to recruit the other brain regions necessary for successful memory encoding.

In addition to memory effects on frontal midline theta, perhaps the most striking oscillatory memory effect was increased beta (~16 Hz; 100–300 ms post stimulus) for LF compared with LR stimuli. Increases in beta power have been observed at the cessation of sensory stimulation [for example, Stevenson et al., 2011], with this beta bounce-back phenomenon hypothesized to represent a refractory gating period during which sensory processes are inhibited. Increased beta power could speculatively prevent memory encoding. No SM effects were observed in the gamma band in the current study. While gamma effects have been observed during working memory using EEG/fMRI [Michels et al., 2010], robust and accurate measurement of this low amplitude signal is complicated by acquiring EEG within the scanner. Investigation of the putative relationship between theta phase and gamma amplitude [Canolty et al., 2006]—which complements theories of memory formation [Lisman and Idiart, 1995]—and investigation of concomitant hemodynamic fluctuation is nevertheless an important objective for future EEG/fMRI-based memory research.

Investigation of BOLD correlates of encoding revealed patterns of task-induced activation and deactivation broadly unaffected by SM performance. A previous positron emission tomography study reported increased activity in regions including ACC, IFG, parahippocampal gyrus, and inferior parietal lobule (IPL) during encoding [Fujii et al., 2002]. These regions were similarly activated in response to encoding stimuli during this study.

Significant activation of the cingulate cortex (BA32) and anterior insula/IFG was observed in response to encoding stimuli. Current models of directed task performance suggest that these regions together comprise a coherent network, whose activity indexes the orientation, maintained vigilance, and higher-order executive processes fundamental to goal-directed task performance [Dosenbach et al., 2006]. It has been proposed that together these regions make up a "salience network," responding to stimuli on the basis of their cognitive, emotional, or homeostatic salience [Seeley et al., 2007]. Given this theoretical function, it is perhaps surprising that activity here did not predict SM performance. It is, however, consistent with previous findings of coherent activity in this network following passive sensory stimulation [White et al., 2010] and may suggest that salience in this broad sense need not be consciously perceived.

It has been proposed that the salience network enables the brain to switch between external and internal

TABLE III. Clusters significantly inversely predicted by theta during encoding

Contrast	Region (Brodmann area)	MNI coordinates (*x*,*y*,*z*)	Peak *T*-value	FWE-corrected *P*-value
LR	Medial frontal cortex (10)	−6,44, 8	8.20	9×10^{-7}
LR<LF	Medial frontal cortex (10)	−10, 48, 10	5.05	1×10^{-4}

Cluster significance shown for clusters present at a voxel-level uncorrected threshold of $P < 0.01$.

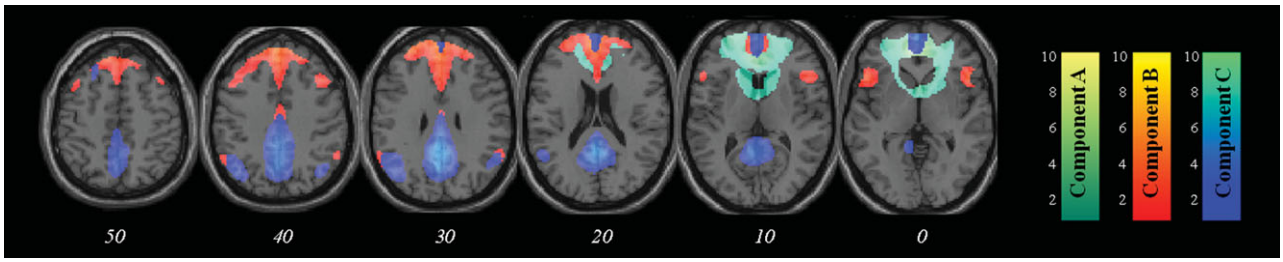

Figure 5.

Independent components with significant spatial correspondence with the default mode network from GIFT. T-distribution maps are overlaid on a standard T1-weighted MR image. The left colorbar depicts *Z*-scores for component A, middle for component B and right for component C. All maps are thresholded at $Z = 1.5$. Italicized numbers below each slice show its MNI Z co-ordinate. [Color figure can be viewed in the online issue, which is available at wileyonlinelibrary.com.]

monitoring systems of function [Sridharan et al., 2008]. In the task used here, it potentially acts to enhance the suppression of certain regions during the encoding of stimuli. Frontal midline, posterior cingulate, precuneus, and bilateral angular gyrus were deactivated during encoding of both LR and LF pictures. These regions together make up the DMN, task-induced deactivation of which is a robust feature of fMRI data [Raichle et al., 2001]. No significant difference in DMN deactivation was observed according to SM performance. However, Anticevic et al. [2010] reported performance-related deactivation of DMN during working memory, with increased DMN deactivation at times of efficacious encoding. The absence of this effect in the current data may perhaps best be explained by differences in the respective tasks. While individual trials are temporally distinct within a Sternberg task, it is possible that the ongoing nature of the experimental task used here may render the Sternberg a more sensitive tool for probing this phenomenon.

Encoding-related activation in medial temporal lobe structures was limited to the parahippocampal gyrus. While activation of additional medial temporal lobe structures such as hippocampus may have been predicted in view of their putative memory function, its absence here can be explained by a previous fMRI report which suggested that these structures are more activated during retrieval than encoding of stimuli [Mandzia et al., 2004]. Furthermore, in light of the notion that these medial temporal lobe structures make up a subsystem of the DMN with a proposed function of prospective thought and related visual imagery [Andrews-Hanna et al., 2010; Greicius et al., 2004; Vincent et al., 2008], and the temporal characteristics of the current task, it is possible that these regions were activated throughout the experiment, thus hindering detection of their activation in relation to encoding stimulus presentation.

We were unable to replicate the findings of Cansino and colleagues [2002] who observed increased BOLD activation

TABLE IV. Default mode network (DMN) stimulus presentation and theta effects

	Encoding stimuli: main effects					
	Later remembered			Later forgotten		
Component	Beta	*T*	*P*	Beta	*T*	*P*
(a) Relationship between encoding stimuli presentation and DMN BOLD activity						
A	−1.48 (0.27)	−5.39	1×10^{-4}	−1.24 (0.20)	−3.276	3×10^{-5}
B	−1.06 (0.30)	−3.51	0.004	−0.65 (0.30)	−2.316	0.047
C	−0.98 (0.24)	−4.13	0.001	−0.57 (0.28)	−3.71	0.069
(a) Relationship between encoding stimuli theta power and DMN BOLD activity						
A	−0.20 (0.11)	−1.84	0.089	−0.03 (0.29)	−0.099	0.922
B	−0.44 (0.14)	−3.09	0.009	0.08 (0.27)	0.286	0.779
C	−0.35 (0.15)	−2.27	0.041	0.12 (0.26)	0.460	0.653

Beta values represent the relationship between DMN BOLD activity and (a) main effect of stimulus; and (b) parametric modulator values for theta. Beta values are taken from the GLM including both convolved task effects and theta parametric modulators. T-values denote results from one sample T-tests of the beta values in the whole group. All T-tests were performed with 13 degrees of freedom. P-values are two-tailed. Bracketed values denote standard error of the mean.

for LR compared to LF pictures in regions including right lateral occipital cortex, left superior temporal gyrus and left IFG. While these previous observations are credible and the current negative finding may reflect nothing more than a lack of power, there are also many situations in which there is imperfect mapping of measured changes in neuronal activity and overt behavior, and as such an improvement in task performance is not universally accompanied by increased BOLD activity. Task practice, for example, robustly attenuates BOLD increases [Koch et al., 2006; Landau et al., 2004; Van Raalten et al., 2008], in a manner which has been shown to bear little relationship to behavior [Landau et al., 2004]. It is also relevant that in certain situations an elevated BOLD response has been evinced as indicative of increased inefficiency of response. It is well established that at low working-memory loads individuals with schizophrenia exhibit increased BOLD activity compared to controls in regions including the dorsolateral prefrontal cortex and ACC [Callicott et al., 2000; Glahn et al., 2005; Manoach et al., 1997, 1999]. These increases are believed to represent a mechanism by which these individuals compensate for inefficiencies of neuronal function - allocating increased resources, while achieving lower or comparable accuracy [Callicott et al., 2000]. EEG reflects activity within neural ensembles that is synchronous on a millisecond time scale [Buzsaki, 2006], whereas this is not necessarily true of the BOLD signal. If during LR trials, neural activity in task-relevant brain regions is precisely synchronized, it would be expected that the magnitude of the BOLD signal would correlate with the magnitude of EEG oscillations. On the other hand, in LF trials, poorly synchronized activity would be expected to make a greater contribution to the BOLD signal. The BOLD signal averaged across trials might be no less in LF trials, but the correlation with EEG oscillations would be lower. Thus, concurrent EEG/fMRI might provide an indication of the degree to which local neural activity is precisely synchronized.

A principal finding of this article is of an inverse relationship between theta and DMN BOLD activity during encoding. This effect is independently observed in analyses using GLMs applied to univariate whole-head voxel data and GLMs applied to multivariate independent component data (Figs. 4 and 5). These findings appear to confirm several correlation analyses of local oscillatory and BOLD responses. Scheeringa et al. [2008, 2009] previously reported anticorrelation of frontal theta and DMN BOLD signal during rest and working memory using EEG/fMRI. Niessing et al. [2005] reported a negative relationship between low frequency (delta and theta) local field potential oscillations measured in cat primary visual cortex and BOLD activity in the same region during the presentation of a grating stimulus. Mukamel et al. [2005] reported a similar phenomenon in human auditory cortex: BOLD activity negatively correlated with low frequency field potentials and positively correlated with gamma. Kilner et al. [2005] suggested that local BOLD activity is a function of the spectral profile of neuro-electric activity. A shift of local activity from predominantly low to predominantly high frequency causes increased energy dissipation and associated increased BOLD activation, while the converse shift is less energetically demanding therefore producing a relatively decreased BOLD response. In an EEG/fMRI study of theta in working memory, Scheeringa et al. [2008] identified the ACC node of the DMN as the most likely theta source, and further suggested that activity in this region modulates the activity in the rest of the coherent network. Beamformer and distributed source models also point to this DMN region [Ishii et al., 1999; Miwakeichi et al., 2004]. On the basis of these findings, it is likely that the frontal theta recorded currently has a medial frontal DMN source.

Localized, event-related synchronization of alpha oscillations has been observed over nontask-relevant brain regions at times when a learnt response is purposefully withheld [Klimesch et al., 1997]. This, coupled with the finding that widespread event-related desynchronization of alpha follows release of this top-down control [Sauseng et al., 2005], lends support to the theory that the alpha signal carries information with respect to current top-down inhibitory state [Klimesch et al., 2007]. It is plausible that an analogous mechanism is discernible in the theta range, permitting theta to modulate DMN activity in a contextually relevant manner.

Our findings from the whole-head univariate analysis imply that the strongest negative relationship between theta power and DMN BOLD signal is found in the medial frontal node of the DMN. The maximal inverse theta relationship with BOLD is observed in medial frontal gyrus (Fig. 4a; Table III) for LR pictures and it is here that the most significant SM effect is observed (Fig. 4b). The ICA findings suggest an inverse relationship between theta modulation and activity in the three DMN components which all have positive loadings over medial frontal regions (Fig. 5; Table IV). It has recently been suggested that the DMN comprises a core system with hubs in these anterior medial prefrontal and medial parietal cortices [Andrews-Hanna et al., 2010]. It has also been proposed that this core system interacts with two functionally and anatomically distinct subsystems: one termed the "dorsal medial PFC subsystem" comprising dorsal medial PFC and temporoparietal junction; and the other "medial temporal lobe system" comprising ventral PFC, posterior IPL, hippocampal formation, and retrosplenial cortex [Andrews-Hanna et al., 2010; Buckner et al., 2009]. The frontal focus of components A and C and the site of the univariate inverse correlation with theta for LR pictures map well onto the anterior medial PFC hub. Tract-tracing reveals that the rhesus monkey homologue of this region has connections with regions including ventro- and dorsomedial PFC, PCC and retrosplenial cortex [Barbas et al., 1999]. This region has also been shown to exhibit high levels of both local and long distance functional connectivity [Sepulcre et al., 2010]. There is therefore support for the

notion that frontal midline theta exerts a suppressive effect on medial PFC which is then transmitted to other DMN regions.

In both the whole-head univariate (Fig. 4; Table III) and spatial ICA (Table IV) analyses, event-related theta signal significantly modulated the relationship between the trial event and BOLD signal during LR trials but exerted a significantly less strong modulatory effect during LF trials. (Consistent findings are also presented in Supporting Information 1 and Supporting Information Figure 1, which report the relationship between BOLD and theta in a component identified using temporal ICA of the EEG data.) Our results suggest that successful storage in memory depends on the relevant neural events occurring at the right time (on a millisecond scale) in addition to the right location. The lack of significant main effect of trial type in predicting BOLD is consistent with the expectation that BOLD signal is not sensitive to the precise timing of neural events, and hence BOLD signal itself is a relatively poor predictor of successful storage in memory. As a caveat to these results it should be stated that the number of trials contributing to the LR and LF conditions differed, as more stimuli were correctly remembered than forgotten. This potentially reduces the power to detect a relationship between theta and DMN activity for LF trials. A more cognitively challenging task could potentially reduce this trial-number imbalance. Furthermore, these analyses assess linear theta-BOLD relationships. While this approach is justified on the basis of previous studies consistently reporting linear relationships between frontocentral theta and medial prefrontal BOLD at rest [Scheeringa et al., 2008] and during working memory performance [Michels et al., 2010; Scheeringa et al., 2009], it is also possible that differences in nonlinear contributions could lead to a difference in the goodness of fit to the linear model for the LR and LF trial types.

Theta source localization using beamforming techniques provides a feasible means of further investigating this SM difference in the inverse theta-DMN relationship. However, the application of a beamformer to the current dataset is considered suboptimal on account of the relatively small number of data channels and reduction in data dimensionality caused by the EEG preprocessing artifact-rejection procedures. Together these factors reduce the interference rejection properties of the beamformer. Future work would be improved by the optimization of experimental design for this purpose [Brookes et al., 2008] and application of eigenspace beamformers to address these issues [Sekihara et al., 2002].

This work, in agreement with several other recent publications [Michels et al., 2010; Scheeringa et al., 2009], highlights the potential of EEG/fMRI for studying relationships between task-modulated, event-related oscillatory activity and regional hemodynamic responses. In demonstrating that the inverse relationship between theta and DMN response is less significant for LF compared with LR items, it provides evidence that disturbance of this relationship underlies poor memory performance. The observed primacy of the medial frontal region of the DMN in this relationship furthers our understanding of functional specialization within the DMN. It is evident that theta oscillations play a crucial role, not only in the recruitment of task-relevant structures, but also in the dampening of processes which may otherwise obstruct goal-directed brain function.

REFERENCES

Allen PJ, Josephs O, Turner R (2000): A method for removing imaging artifact from continuous EEG recorded during functional MRI. Neuroimage 12:230–239.

Allen PJ, Polizzi G, Krakow K, Fish DR, Lemieux L (1998): Identification of EEG events in the MR scanner: The problem of pulse artifact and a method for its subtraction. Neuroimage 8:229–239.

Andrews-Hanna JR, Reidler JS, Sepulcre J, Poulin R, Buckner RL (2010): Functional-anatomic fractionation of the brain's default network. Neuron 65:550–562.

Anticevic A, Repovs G, Shulman GL, Barch DM (2010): When less is more: TPJ and default network deactivation during encoding predicts working memory performance. Neuroimage 49:2638–2648.

Barbas H, Ghashghaei H, Dombrowski SM, Rempel-Clower NL. (1999): Medial prefrontal cortices are unified by common connections with superior temporal cortices and distinguished by input from memory-related areas in the rhesus monkey. J Comp Neurol 410:343–367.

Brewer JB, Zhao Z, Desmond JE, Glover GH, Gabrieli JD (1998): Making memories: Brain activity that predicts how well visual experience will be remembered. Science 281:1185–1187.

Brookes MJ, Vrba J, Robinson SE, Stevenson CM, Peters AM, Barnes GR, Hillebrand A, Morris PG (2008): Optimising experimental design for MEG beamformer imaging. Neuroimage 39:1788–1802.

Buckner RL, Andrews-Hanna JR, Schacter DL (2008): The brain's default network: Anatomy, function, and relevance to disease. Ann NY Acad Sci 1124:1–38.

Buckner RL, Sepulcre J, Talukdar T, Krienen FM, Liu H, Hedden T, Andrews-Hanna JR, Sperling RA, Johnson KA (2009): Cortical hubs revealed by intrinsic functional connectivity: Mapping, assessment of stability, and relation to Alzheimer's disease. J Neurosci 29:1860–1873.

Buzsaki G, Draguhn A (2004): Neuronal oscillations in cortical networks. Science 304:1926–1929.

Buzsaki G (2006): Rhythms of the Brain. UK: Oxford University Press.

Callicott JH, Bertolino A, Mattay VS, Langheim FJ, Duyn J, Coppola R, Goldberg TE, Weinberger DR (2000): Physiological dysfunction of the dorsolateral prefrontal cortex in schizophrenia revisited. Cereb Cortex 10:1078–1092.

Canli T, Zhao Z, Brewer J, Gabrieli JD, Cahill L (2000): Event-related activation in the human amygdala associates with later memory for individual emotional experience. J Neurosci 20:RC99.

Canolty RT, Edwards E, Dalal SS, Soltani M, Nagarajan SS, Kirsch HE, Berger MS, Barbaro NM, Knight RT (2006): High gamma power is phase-locked to theta oscillations in human neocortex. Science 313:1626–1628.

Cansino S, Maquet P, Dolan RJ, Rugg MD (2002): Brain activity underlying encoding and retrieval of source memory. Cereb Cortex 12:1048–1056.

Chia JM, Fischer SE, Wickline SA, Lorenz CH (2000): Performance of QRS detection for cardiac magnetic resonance imaging with a novel vectorcardiographic triggering method. J Magn Reson Imaging 12:678–688.

Corbetta M, Kincade JM, Shulman GL (2002): Neural systems for visual orienting and their relationships to spatial working memory. J Cogn Neurosci 14:508–523.

Daselaar SM, Prince SE, Cabeza R (2004): When less means more: Deactivations during encoding that predict subsequent memory. Neuroimage 23:921–927.

Delorme A, Makeig S (2004): EEGLAB: An open source toolbox for analysis of single-trial EEG dynamics including independent component analysis. J Neurosci Methods 134:9–21.

Dosenbach NU, Visscher KM, Palmer ED, Miezin FM, Wenger KK, Kang HC, Burgund ED, Grimes AL, Schlaggar BL, Petersen SE (2006): A core system for the implementation of task sets. Neuron 50:799–812.

Fujii T, Okuda J, Tsukiura T, Ohtake H, Suzuki M, Kawashima R, Itoh M, Fukuda H, Yamadori A (2002): Encoding-related brain activity during deep processing of verbal materials: A PET study. Neurosci Res 44:429–438.

Gevins A, Smith ME, McEvoy L, Yu D (1997): High-resolution EEG mapping of cortical activation related to working memory: Effects of task difficulty, type of processing, and practice. Cereb Cortex 7:374–385.

Glahn DC, Ragland JD, Abramoff A, Barrett J, Laird AR, Bearden CE, Velligan DI (2005): Beyond hypofrontality: A quantitative meta-analysis of functional neuroimaging studies of working memory in schizophrenia. Hum Brain Mapp 25:60–69.

Glover GH, Li TQ, Ress D (2000): Image-based method for retrospective correction of physiological motion effects in fMRI: RETROICOR. Magn Reson Med 44:162–167.

Gowland PA, Bowtell R (2007): Theoretical optimization of multi-echo fMRI data acquisition. Phys Med Biol 52:1801–1813.

Greicius MD, Srivastava G, Reiss AL, Menon V (2004): Default-mode network activity distinguishes Alzheimer's disease from healthy aging: evidence from functional MRI. Proc Natl Acad Sci USA 101:4637–4642.

Gruber T, Tsivilis D, Giabbiconi CM, Muller MM (2008): Induced electroencephalogram oscillations during source memory: Familiarity is reflected in the gamma band, recollection in the theta band. J Cogn Neurosci 20:1043–1053.

Jensen O, Tesche CD (2002): Frontal theta activity in humans increases with memory load in a working memory task. Eur J Neurosci 15:1395–1399.

Kelley WM, Miezin FM, McDermott KB, Buckner RL, Raichle ME, Cohen NJ, Ollinger JM, Akbudak E, Conturo TE, Snyder AZ, Petersen SE (1998): Hemispheric specialization in human dorsal frontal cortex and medial temporal lobe for verbal and nonverbal memory encoding. Neuron 20:927–936.

Kilner JM, Mattout J, Henson R, Friston KJ (2005): Hemodynamic correlates of EEG: A heuristic. Neuroimage 28:280–286.

Kiselev VG, Posse S (1999): Analytical model of susceptibility-induced MR signal dephasing: Effect of diffusion in a microvascular network. Magn Reson Med 41:499–509.

Klimesch W, Doppelmayr M, Schimke H, Ripper B (1997): Theta synchronization and alpha desynchronization in a memory task. Psychophysiology 34:169–176.

Klimesch W, Sauseng P, Hanslmayr S (2007): EEG alpha oscillations: The inhibition-timing hypothesis. Brain Res Rev 53:63–68.

Koch K, Wagner G, von Consbruch K, Nenadic I, Schultz C, Ehle C, Reichenbach J, Sauer H, Schlosser R (2006): Temporal changes in neural activation during practice of information retrieval from short-term memory: An fMRI study. Brain Res 1107:140–150.

Landau SM, Schumacher EH, Garavan H, Druzgal TJ, D'Esposito M (2004): A functional MRI study of the influence of practice on component processes of working memory. Neuroimage 22:211–221.

Lisman JE, Idiart MA (1995): Storage of 7 /- 2 short-term memories in oscillatory subcycles. Science 267:1512–1515.

Luu P, Tucker DM (2001): Regulating action: Alternating activation of midline frontal and motor cortical networks. Clin Neurophysiol 112:1295–1306.

Makeig S (1993): Auditory event-related dynamics of the EEG spectrum and effects of exposure to tones. Electroencephalogr Clin Neurophysiol 86:283–293.

Makeig S, Delorme A, Westerfield M, Jung TP, Townsend J, Courchesne E, Sejnowski TJ (2004): Electroencephalographic brain dynamics following manually responded visual targets. PLoS Biol 2:e176.

Mandelkow H, Halder P, Boesiger P, Brandeis D (2006): Synchronization facilitates removal of MRI artefacts from concurrent EEG recordings and increases usable bandwidth. Neuroimage 32:1120–1126.

Mandzia JL, Black SE, McAndrews MP, Grady C, Graham S (2004): fMRI differences in encoding and retrieval of pictures due to encoding strategy in the elderly. Hum Brain Mapp 21:1–14.

Manoach DS, Press DZ, Thangaraj V, Searl MM, Goff DC, Halpern E, Saper CB, Warach S (1999): Schizophrenic subjects activate dorsolateral prefrontal cortex during a working memory task, as measured by fMRI. Biol Psychiatry 45:1128–1137.

Manoach DS, Schlaug G, Siewert B, Darby DG, Bly BM, Benfield A, Edelman RR, Warach S (1997): Prefrontal cortex fMRI signal changes are correlated with working memory load. Neuroreport 8:545–549.

McKiernan KA, Kaufman JN, Kucera-Thompson J, Binder JR (2003): A parametric manipulation of factors affecting task-induced deactivation in functional neuroimaging. J Cogn Neurosci 15:394–408.

Michels L, Bucher K, Luchinger R, Klaver P, Martin E, Jeanmonod D, Brandeis D (2010): Simultaneous EEG-fMRI during a working memory task: Modulations in low and high frequency bands. PLoS One 5:e10298.

Mukamel R, Gelbard H, Arieli A, Hasson U, Fried I, Malach R (2005): Coupling between neuronal firing, field potentials, and FMRI in human auditory cortex. Science 309:951–954.

Mullinger KJ, Morgan PS, Bowtell RW (2008): Improved artifact correction for combined electroencephalography/functional MRI by means of synchronization and use of vectorcardiogram recordings. J Magn Reson Imaging 27:607–616.

Murdock BB Jr (1960): The distinctiveness of stimuli. Psychol Rev 67:16–31.

Niazy RK, Beckmann CF, Iannetti GD, Brady JM, Smith SM (2005): Removal of FMRI environment artifacts from EEG data using optimal basis sets. Neuroimage 28:720–737.

Niessing J, Ebisch B, Schmidt KE, Niessing M, Singer W, Galuske RA (2005): Hemodynamic signals correlate tightly with synchronized gamma oscillations. Science 309:948–951.

Onton J, Delorme A, Makeig S (2005): Frontal midline EEG dynamics during working memory. Neuroimage 27:341–356.

Osipova D, Takashima A, Oostenveld R, Fernandez G, Maris E, Jensen O (2006): Theta and gamma oscillations predict encoding and retrieval of declarative memory. J Neurosci 26:7523–7531.

Otten LJ, Rugg MD (2001): When more means less: Neural activity related to unsuccessful memory encoding. Curr Biol 11:1528–1530.

Paller KA, Wagner AD (2002): Observing the transformation of experience into memory. Trends Cogn Sci 6:93–102.

Paus T (2001): Primate anterior cingulate cortex: Where motor control, drive and cognition interface. Nat Rev Neurosci 2:417–424.

Paus T, Petrides M, Evans AC, Meyer E (1993): Role of the human anterior cingulate cortex in the control of oculomotor, manual, and speech responses: A positron emission tomography study. J Neurophysiol 70:453–469.

Posse S, Wiese S, Gembris D, Mathiak K, Kessler C, Grosse-Ruyken ML, Elghahwagi B, Richards T, Dager SR, Kiselev VG (1999): Enhancement of BOLD-contrast sensitivity by single-shot multi-echo functional MR imaging. Magn Reson Med 42:87–97.

Raichle ME, MacLeod AM, Snyder AZ, Powers WJ, Gusnard DA, Shulman GL (2001): A default mode of brain function. Proc Natl Acad Sci USA 98:676–682.

Rutishauser U, Ross IB, Mamelak AN, Schuman EM (2010): Human memory strength is predicted by theta-frequency phase-locking of single neurons. Nature 464:903–907.

Sauseng P, Klimesch W, Freunberger R, Pecherstorfer T, Hanslmayr S, Doppelmayr M (2006): Relevance of EEG alpha and theta oscillations during task switching. Exp Brain Res 170:295–301.

Sauseng P, Hoppe J, Klimesch W, Gerloff C, Hummel FC (2007): Dissociation of sustained attention from central executive functions: Local activity and interregional connectivity in the theta range. Eur J Neurosci 25:587–593.

Scheeringa R, Bastiaansen MC, Petersson KM, Oostenveld R, Norris DG, Hagoort P (2008): Frontal theta EEG activity correlates negatively with the default mode network in resting state. Int J Psychophysiol 67:242–251.

Scheeringa R, Petersson KM, Oostenveld R, Norris DG, Hagoort P, Bastiaansen MC (2009): Trial-by-trial coupling between EEG and BOLD identifies networks related to alpha and theta EEG power increases during working memory maintenance. Neuroimage 44:1224–1238.

Sederberg PB, Kahana MJ, Howard MW, Donner EJ, Madsen JR (2003): Theta and gamma oscillations during encoding predict subsequent recall. J Neurosci 23:10809–10814.

Sekihara K, Nagarajan SS, Poeppel D, Marantz A, Miyashita Y (2002): Application of an MEG eigenspace beamformer to reconstructing spatio-temporal activities of neural sources. Hum Brain Mapp 15:199–215.

Seeley WW, Menon V, Schatzberg AF, Keller J, Glover GH, Kenna H, Reiss AL, Greicius MD (2007): Dissociable intrinsic connectivity networks for salience processing and executive control. J Neurosci 27:2349–2356.

Sepulcre J, Liu H, Talukdar T, Martincorena I, Yeo BT, Buckner RL (2010): The organization of local and distant functional connectivity in the human brain. PLoS Comput Biol 6:e1000808.

Spaniol J, Davidson PS, Kim AS, Han H, Moscovitch M, Grady CL (2009): Event-related fMRI studies of episodic encoding and retrieval: Meta-analyses using activation likelihood estimation. Neuropsychologia 47(8–9):1765–1779.

Sridharan D, Levitin DJ, Menon V (2008): A critical role for the right fronto-insular cortex in switching between central-executive and default-mode networks. Proc Natl Acad Sci USA 105:12569–12574.

Stevenson CM, Brookes MJ, Morris PG (2011): β-Band correlates of the fMRI BOLD response. Hum Brain Mapp 32:182–97.

Tort AB, Komorowski RW, Manns JR, Kopell NJ, Eichenbaum H (2009): Theta-gamma coupling increases during the learning of item-context associations. Proc Natl Acad Sci USA 106:20942–20947.

Van Raalten TR, Ramsey NF, Duyn J, Jansma JM (2008): Practice induces function-specific changes in brain activity. PLoS One 3:e3270.

von Stein A, Sarnthein J (2000): Different frequencies for different scales of cortical integration: From local gamma to long range alpha/theta synchronization. Int J Psychophysiol 38:301–313.

Wagner AD, Poldrack RA, Eldridge LL, Desmond JE, Glover GH, Gabrieli JD (1998): Material-specific lateralization of prefrontal activation during episodic encoding and retrieval. Neuroreport 9:3711–3717.

Weidemann CT, Mollison MV, Kahana MJ (2009): Electrophysiological correlates of high-level perception during spatial navigation. Psychon Bull Rev 16:313–319.

Weiss S, Muller HM, Rappelsberger P (2000): Theta synchronization predicts efficient memory encoding of concrete and abstract nouns. Neuroreport 11:2357–2361.

White TP, Joseph V, Francis ST, Liddle PF (2010): Aberrant salience network (bilateral insula and anterior cingulate cortex) connectivity during information processing in schizophrenia. Schizophr Res 123:105–115.